Environmental Science & Technology Letters

pubs.acs.org/journal/estlcu

Letter

COVID-19 Lockdowns Afford the First Satellite-Based Confirmation That Vehicles Are an Under-recognized Source of Urban NH_3 Pollution in Los Angeles

Hansen Cao, Daven K. Henze,* Karen Cady-Pereira, Brian C. McDonald, Colin Harkins, Kang Sun, Kevin W. Bowman, Tzung-May Fu, and Muhammad O. Nawaz

Cite This: *Environ. Sci. Technol. Lett.* 2022, 9, 3−9

Read Online

ACCESS | Metrics & More | Article Recommendations | Supporting Information

ABSTRACT: In situ measurements have suggested vehicle emissions may dominate agricultural sources of NH_3 in many cities, which is alarming given the potential for urban NH_3 to significantly increase human exposure to ambient particulate matter. However, confirmation of the prevalence of vehicle NH_3 throughout a city has been challenging because of mixing with agricultural sources, and the latter are thus routinely assumed to dominate. Here we report vehicle NH_3 emissions based on TROPOMI NO_2 and CrIS NH_3 (0.152 kg s^{-1}) that are consistent with a model-based estimate (0.178 kg s^{-1}) and show that COVID-19 lockdowns provide a unique opportunity for making the first satellite-based constraints on vehicle NH_3 emissions for an entire urban region (western Los Angeles), which we find make up 60−95% of total NH_3 emissions, substantially higher than the values of 13−22% in state and national inventories. This provides a new means of constraining a component of transportation emissions whose impacts may rival those of NO_x yet which has been largely under-recognized and uncontrolled.

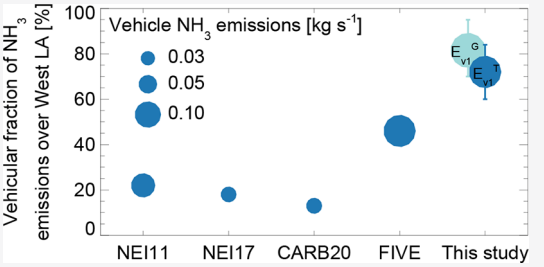

INTRODUCTION

Atmospheric ammonia contributes to ambient air pollution primarily through formation of inorganic components (ammonium sulfate and ammonium nitrate) of fine particulate matter ($PM_{2.5}$). While the largest sources of NH_3 are agricultural at national to global scales,[1] NH_3 is also emitted from vehicles. In light- and medium-weight vehicles using catalytic converters, the air-rich fuel ratios that are optimal for reducing emissions of NO_x produce NH_3 emissions.[2−4] More recently, diesel engines of heavy duty vehicles use urea for selective catalytic reduction (SCR), leading to NH_3 emissions.[5] Emissions of NH_3 in urban areas are of concern because of the efficient formation of ammonium nitrate in NO_x-rich environments and the potential for exposing large populations to $PM_{2.5}$; for example, in the United States, despite vehicle emissions being more than an order of magnitude smaller than agricultural emissions, they are estimated to lead to similar numbers of premature deaths (~15,000) per year.[6,7]

There is, however, considerable discussion around the magnitude of vehicle NH_3 emissions in the United States and internationally. Early studies identified emissions from light and heavy duty vehicles equipped with catalytic converters as a missing source in inventories[3,8,9] and potentially a dominant source of NH_3 in urban environments worldwide.[10−13] Other work has found more limited evidence of vehicle NH_3 emissions in urban environments.[14,15] However, many of these studies predate the adoption of SCR systems by heavy duty vehicles that has led to increasing NH_3 emissions.[16] More recent research suggests U.S. vehicular NH_3 emissions are actually twice as high as national inventories.[17−21] Evidence for vehicle NH_3 emissions has come from field measurements near roadways or in tunnels using isotope signatures[21−23] or correlations of NH_3 with combustion tracers such as CO, CO_2, and NO_x,[19,24−26] from laboratory studies using chassis dynamometers,[4,27] and from open-path mobile measurements[28,29] of in-use vehicle operations over a range of conditions.[19]

A challenge with characterizing vehicle emissions over an entire metropolitan area is reconciling emission factors that vary on the basis of vehicle age, road grade, temperature, and operating conditions. Inverse modeling approaches based on ambient concentration are appealing in this regard. Top-down estimates of vehicle emissions of NH_3 throughout western Los Angeles (LA) were first made using NH_3 and CO measurements from aircraft.[30] While remote-sensing instruments have been used to identify NH_3 emissions from agriculture,[31,32] industry and fertilizer production,[33] biomass burning,[34] and other natural sources,[35] there has not yet been a satellite-based

Received: September 8, 2021
Revised: November 5, 2021
Accepted: November 8, 2021
Published: November 23, 2021

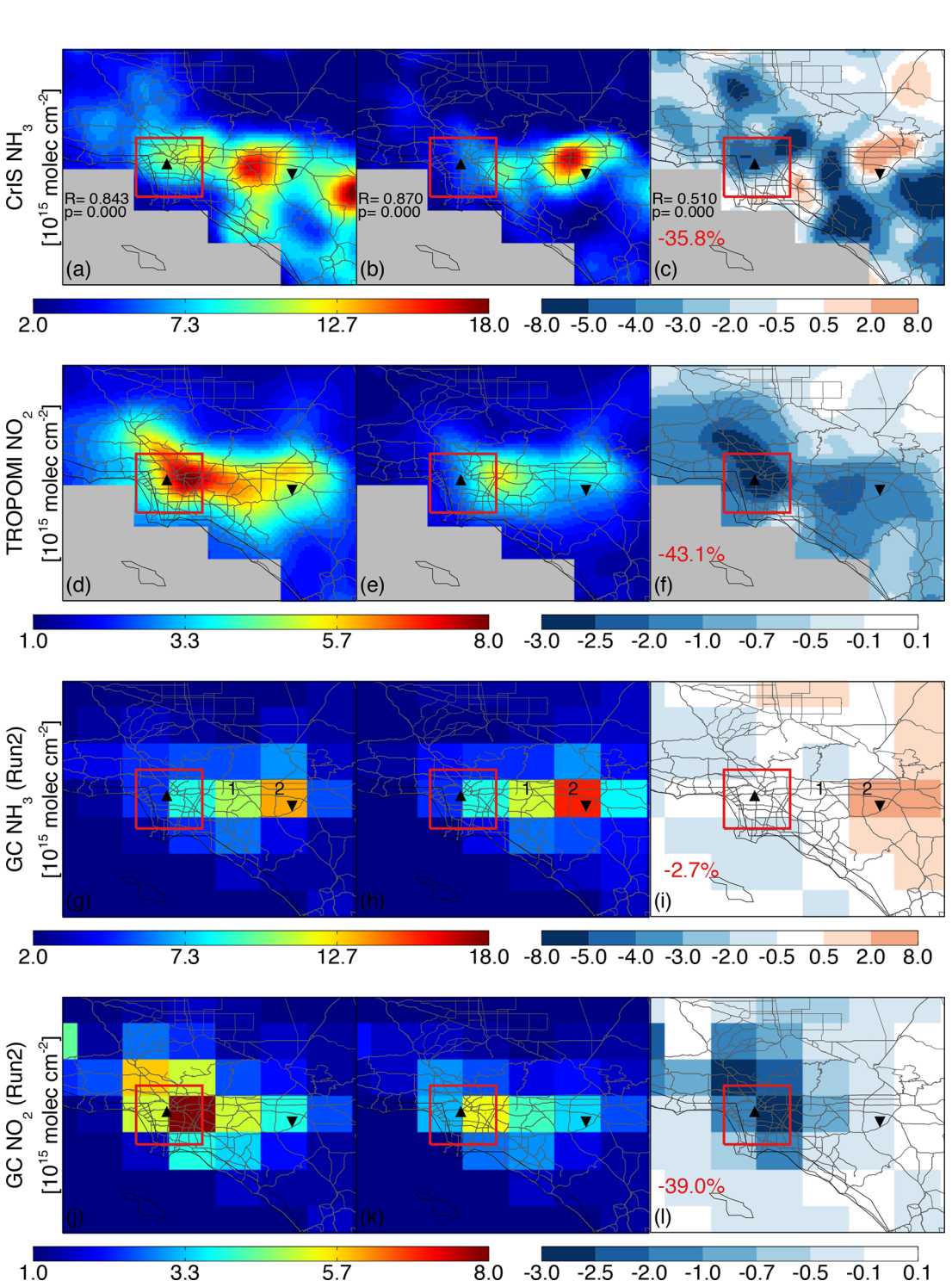

Figure 1. CrIS NH_3 column concentrations (a) during March 1−15 and (b) during March 16−31, as well as (c) their difference (difference = (b) − (a)). (d−f) Same as panels (a)−(c), respectively, but for TROPOMI NO_2 column concentrations (qa > 0.75). (g−i) Same as panels (a)−(c), respectively, but for GC-simulated NH_3 column concentrations from Run2 (see Table S1 and Text S2). (j−l) Same as panels (a)−(c), respectively, but for GEOS-Chem-simulated NO_2 column concentrations from Run2 (see Table S1 and Text S2). *R* is the spatial correlation coefficient between CrIS NH_3 and TROPOMI NO_2 columns within the red box in each period; *p* is the corresponding significance level. The red box defines the western LA domain (33.80−34.20°N, 118.50−118.05°W) on which we focus in this study. The red numbers in panels (c), (f), (i), and (l) are percentage decreases of NH_3 and NO_2 columns within western LA between these two periods observed by CrIS and TROPOMI and simulated by GEOS-Chem, respectively. The upward (△) and downward (▽) triangles indicate the locations of the downtown LA site and Riverside Municipal ARPT site, respectively, in Figure S2.

https://doi.org/10.1021/acs.estlett.1c00730
Environ. Sci. Technol. Lett. 2022, 9, 3−9

measurement of NH_3 specifically linked to transportation emissions. A difficulty is that transportation and other urban non-agricultural sources (e.g., emissions from industrial and residential sources and domestic animals) are located near one another; NH_3 from these sources also does not have distinct seasonalities,[36] making them difficult to deconvolve from ambient concentrations.

The drastic reductions in traffic associated with COVID-19 lockdowns in the spring of 2020 provide a unique opportunity to examine the impact of transportation emissions on atmospheric composition. Here we focus on LA, where previous assessments have pointed toward underestimated vehicle NH_3 emissions,[18,30] and we analyze how satellite observations of both NH_3 and NO_2 may be used to constrain NH_3 from this sector. Apart from meteorological impacts,[37] changes in NO_2 concentrations are mainly linked to changes in traffic during the lockdown, as the main source of NO_x in this region is on-road transportation. We examine how correlations of these signals with NH_3 concentrations, along with considerations of changes in meteorology, may be used to quantify the changes in transportation NH_3 emissions associated with the lockdown. Using changes in traffic activity, we then estimate the total NH_3 vehicle emissions under normal (nonlockdown) conditions. To evaluate this new approach, we also conduct chemical transport model simulations (to account for the role of changing meteorology and NH_3 lifetime) and use these to estimate vehicle NH_3 emissions from the satellite observations of NH_3. Finally, we compare the top-down vehicle NH_3 emissions between these two approaches and to previous and current bottom-up estimates.

MATERIALS AND METHODS

We examine vehicle NH_3 emissions in LA before and during the COVID-19 lockdown using satellite observations of NH_3 from CrIS[38−40] and NO_2 observations from TROPOMI,[41,42] both of which are processed using a physics-based oversampling method.[43] To extrapolate from changes in emissions during the lockdown to total vehicle emissions prior to lockdown, we use the emission reduction ratios during the lockdown from a new bottom-up mobile transportation inventory based on fuel sales, the Fuel-based Inventory of Vehicle Emissions (FIVE).[44−47] Details of these data sets are provided in Text S1. We also examine the role of changes in meteorology during the lockdown using ground-based hourly measurements of air temperature, precipitation, wind speed, and wind direction, which are further described in Text S3 and Figure S2.

To estimate vehicle NH_3 emissions, we use two different approaches: one based on TROPOMI NO_2 and another based on chemical transport modeling with GEOS-Chem. The TROPOMI NO_2 approach exploits the relationship between NO_x and NH_3 co-emitted from vehicles, while the model-based approach utilizes GEOS-Chem to account for impacts from meteorological changes, temperature-driven impacts on agricultural NH_3 emission reduction, and how reduced concentrations of NO_2 impact NH_3 lifetime. Overviews of these methods are provided below, with additional details in Texts S2 and S4.

Changes in Concentrations Observed by Satellites. We first consider NH_3 column concentrations from CrIS and NO_2 column concentrations from TROPOMI over the LA basin in March 2020 (Figure 1). To isolate the impact of the COVID-19 lockdown, we focus on March 1−15 and March 16−31, 2020, representing conditions before and during the onset of the lockdown in LA, respectively (see Text S1 for the rationale behind this choice). Panel (a) shows NH_3 column concentrations prior to the lockdown. While the hot spot to the west of Riverside is known to be caused by livestock,[30,33] here we also identify a smaller yet distinct hot spot over downtown LA. We further note that there are no fertilizer production facilities within this part of LA.[48] In the second half of March (panel (b)), the peak NH_3 concentrations over the basin largely decrease, with the local maxima over the downtown and Riverside regions shifting slightly eastward, and there are smaller-scale, variable fluctuations throughout the basin.

Isolating NH_3 concentrations due to transportation is often complicated by the presence of nearby or overlapping agricultural sources of NH_3. In contrast, NO_2 concentrations in urban areas are dominated by non-agricultural emissions and thus provide a more distinct observation of the impact of transportation changes. Panels (d)−(f) of Figure 1 show TROPOMI NO_2 column concentrations over LA and its surrounding areas during the first and second halves of March and their differences, respectively. During the first period, unlike NH_3 concentrations, NO_2 concentrations exhibit a singular maximum over the downtown LA region and are relatively high across the LA basin, suggesting that total anthropogenic NO_x emissions (vehicle and non-vehicle) are generally high throughout the basin and local anthropogenic NO_x emissions peak in the downtown area. This NO_2 hot spot is co-located with the CrIS NH_3 hot spot over the downtown area ($R = 0.843$), suggesting these come from the same source. During the second period, there are significant decreases of TROPOMI NO_2 column concentrations throughout the basin (especially the downtown area). Like CrIS NH_3, TROPOMI detects an eastward shift of the downtown hot spot. This eastward shift suggests that NO_2 over the downtown area is also impacted by stronger winds from the west direction in the second period (Figure S2 (h)). Overall, the co-location and the similar eastward shift of the TROPOMI NO_2 and CrIS NH_3 hot spots over downtown LA are consistent with them sharing a common source over downtown LA that, given the location, is likely vehicle emissions. We thus focus our analysis on the western LA region shown in the red box, which was selected because CrIS NH_3 and TROPOMI NO_2 measurements have a particularly high spatial correlation there, with R values between 0.843 ($p < 0.001$) and 0.870 ($p < 0.001$) during these two periods.

Estimating Vehicle NH_3 Emissions and Vehicular Fractions. We first consider the difference in CrIS NH_3 column concentrations ($\Delta\Omega = \Omega_2 - \Omega_1$), where Ω_1 and Ω_2 are the area-weighted spatial averages of CrIS NH_3 column concentrations within the western LA box during the first and second periods, respectively. We estimate the contribution to the total change in column concentration owing to changes in vehicle emissions ($\Delta\Omega_v$) and non-vehicle-related factors ($\Delta\Omega_{nv}$),

$$\Delta\Omega = \Delta\Omega_v + \Delta\Omega_{nv} \quad (1)$$

Here the non-vehicle factors include changes in meteorology, reduction in agricultural NH_3 emissions owing to decreased temperatures, and increases in NH_3 lifetime owing to decreased NO_2 concentrations.

https://doi.org/10.1021/acs.estlett.1c00730
Environ. Sci. Technol. Lett. 2022, 9, 3−9

We use two different approaches to calculate $\Delta\Omega_v$ in this study. We first make use of the changes in NO_2 concentrations, which have a distinct transportation signal, as a proxy for changes in vehicle emissions and correlate the remote sensing observations to estimate changes in co-emitted NH_3. As described more completely in Text S2, we use the regression relationship between NO_2 and NH_3 concentrations in the second half of March, and the fraction of total NO_x emissions owing to vehicles in bottom-up inventories, to estimate the change in CrIS NH_3 concentrations owing to vehicles. Alternatively, we use the GEOS-Chem model to quantify how much NH_3 concentrations are expected to have changed owing to factors other than changes in vehicle emissions (i.e., meteorology, decreased agricultural emissions, and increased lifetime); subtracting these model-estimated values from the observed change in total NH_3 provides an alternative estimate of $\Delta\Omega_v$.

Using $\Delta\Omega_v$ from either of these two approaches, we can calculate the corresponding changes in vehicle emissions (ΔE_v) of NH_3 as

$$\Delta E_v = \frac{\Delta\Omega_v}{\overline{\tau}} \tag{2}$$

where $\overline{\tau}$ is the average lifetime during these two periods. While other studies that have directly estimated NH_3 emissions from analysis of satellite NH_3 observations have assumed lifetimes of 1−3 hours,[33,49] here we also use a chemical transport model to estimate the lifetime of NH_3 specifically in this region, which we find to be 3.83 hours on average.

Ultimately, it is of interest to know the NH_3 vehicle emissions prior to the lockdown. From the FIVE inventory, we know the fractional change in vehicle activity between these periods (f, 0.236). Here we assume that emissions factors were constant across these periods (i.e., we neglect changes owing to decreased congestion during the lockdown or changes owing to adjustments of the fleet split between gasoline and diesel vehicles), in which case this value can be used to calculate the vehicle NH_3 emissions prior to the lockdown (E_{v1}) as

$$E_{v1} = \frac{\Delta E_v}{f} \tag{3}$$

Additionally, it is of interest to determine the fraction of NH_3 in urban areas emitted from transportation. For the western LA region, the vehicular percentage of total NH_3 emissions in previous inventories ranges from 13% (CARB 2020) to 22% (NEI 2011), the higher end of which is 2 times lower than in our updated FIVE inventory (46%). However, studies based on in situ measurements have suggested transportation is actually the dominant source of NH_3 in many cities.[19−21] To provide a new top-down perspective on this question, we first calculate the total NH_3 emissions (E_1) in the first period as

$$E_1 = \frac{\Omega_1}{\tau_1} - B_1 \tag{4}$$

where τ_1 is the NH_3 lifetime during the first period, Ω_1/τ_1 is the total NH_3 flux entering the western LA box in the first period, and B_1 is the horizontal NH_3 flux from outside of the western LA box during the first period. While it is hard to precisely estimate the boundary flux, B_1, we can estimate a range based on the difference between the change in CrIS-based total NH_3 flux and the change in vehicle NH_3 emissions between these two periods. This range (see Text S4) is 0 to $0.48E_{v1}$ in the TROPOMI-based approach and 0 to $0.37E_{v1}$ in the model-based approach.

RESULTS AND DISCUSSION

Vehicle NH_3 emissions in western LA in the first half of March 2020 and the corresponding vehicular fraction using both the TROPOMI-based approach (E_{v1}^T) and the model-based approach (E_{v1}^G) are summarized in Table 1. These vehicle

Table 1. Daily Vehicular NH_3 Emission Estimates (kilograms per second) and Vehicular Fractions (%) of the Total Emissions for Western LA

literature	target period	western LA
bottom-up[a]		
FIVE	March 1−15, 2020	0.127
	March 2019	0.150 ± 0.020 (46%)
NEI11	March 2011	0.085 (22%)
NEI17	March 2017	0.036 (18%)
CARB20	March 2020[b]	0.037 (13%)
top-down[c]		
E_{v1}^T	March 1−15, 2020	0.152 (60−84%)
E_{v1}^G (ω = 1.93[d])	March 1−15, 2020	0.178 (70% −95%)

[a]Accounting for only on-road vehicle emissions. [b]Not accounting for COVID-19 lockdown. [c]Ranges of vehicle fractions stem from uncertainty in the horizontal flux of NH_3 in the western LA domain. [d]Wind measurement-based correction factor for simulated meteorology impacts (see Text S3 for details).

NH_3 emission estimates have also been converted to daily average values using the FIVE-based ratio (1.39) of mid-day vehicular emissions to daily vehicular emissions[44] to compare to daily bottom-up inventories. The TROPOMI-based vehicle NH_3 emissions are 0.152 kg s^{-1}, consistent with those derived using a model (0.178 kg s^{-1}). Correspondingly, the ranges of vehicular percentages (60−84% for TROPOMI-based vs 70−95% for model-based) using these two approaches also overlap (within an uncertainty of 17%); this supports the assumption that the high spatial correlation between TROPOMI NO_2 and CrIS NH_3 in this region is owing to shared vehicular emissions.

Uncertainty analysis (Text S5) shows that the TROPOMI-based estimate generally has an uncertainty that is smaller than the model-based estimate because the latter is subject to the accuracy of the simulated meteorological impacts. Homogeneous biases in TROPOMI NO_2 do not impact our top-down vehicle emission estimates (Text S5). Concentration-dependent biases in CrIS NH_3 retrievals could possibly lead to underestimation of vehicle NH_3 emissions and emissions fractions using the model-based approach (see Text S2). Both approaches are subject to the accuracy of the simulated NH_3 lifetime; ranges based on our modeling (4.04 to 3.61 hours) and previous studies (3 to 1 hours) translate directly to −5% to 284% differences in top-down estimates of vehicle emissions (but do not effect vehicle fraction estimates). While collectively these issues make the upper bound on vehicle emissions and vehicle emissions fractions harder to constrain, the lower bound is still significantly higher than prior inventory estimates for both.

Comparison with Other Estimates. We compare the top-down vehicular NH_3 emission estimates to previous and current bottom-up estimates in Table 1. Our top-down vehicular NH_3 emissions (E_{v1}^T and E_{v1}^G) for western LA from

https://doi.org/10.1021/acs.estlett.1c00730
Environ. Sci. Technol. Lett. 2022, 9, 3−9

March 1 to 15 range from 0.152 to 0.178 kg s^{-1}, significantly larger (by 1.8 to 4.9 times, respectively) than the NEI 2011/NEI 2017 vehicular NH_3 emissions of 0.085/0.036 kg s^{-1} and the CARB 2020 emissions of 0.037 kg s^{-1} for the same region. The FIVE 2020 emissions of 0.127 kg s^{-1} and 2019 (0.150 kg s^{-1}) are also much larger than these estimates and approach our top-down estimates. The low biases in bottom-up inventories are likely due to large uncertainties in emission factors and possible leaks of urea from diesel-powered trucks equipped with SCRs. Compared to a previous top-down estimate of 0.72 ± 0.28 kg s^{-1} for a similar region in LA (extending further east and including some of the agricultural hot spot) for May and June 2010 from Nowak et al.[30], our top-down estimate is lower by a factor of 4.0−4.7. The former was obtained by multiplying aircraft-based NH_3:CO ratios by the 2008 CARB inventory CO emissions and is reasonably larger due to the contribution of nontransportation sources (e.g., nearby livestock sources, urban biosphere, etc.).

The vehicular fraction of total NH_3 emissions over western LA in previous inventories ranges from 13% (CARB 2020) to 22% (NEI 2011) and is double the higher range of those values in our updated FIVE inventory (46%). However, studies based on in situ measurements have suggested transportation is actually the dominant source of NH_3 in several cities.[19−21] Consistent with those in situ measurements, our top-down estimates range from 60% to 95%, considerably higher than those of both previous (NEI, CARB) bottom-up inventories. The alternative (FIVE) bottom-up estimate approaches the lower end of our top-down estimates, all of which serves to highlight the dominant role of the vehicular source in total NH_3 emissions in this urban area as reported in previous studies.[19−21]

Implications. Globally, ∼20% of the burden of disease associated with $PM_{2.5}$ exposure is estimated to stem from NH_3 emissions from agriculture.[50] The socio-economic benefits of controlling agricultural NH_3 have been highlighted in studies comparing the cost of mitigating agricultural emissions to the air quality benefits.[51,52] Given the apparent under-recognized magnitude of transportation NH_3 emissions coupled with the potential of this source for contributing to $PM_{2.5}$ exposure in populated areas, re-evaluating the health impacts of transportation emissions is warranted. If these emissions have been severely underestimated by a factor of 1.8−4.9, as the findings of this work support, then the health impacts of vehicle NH_3 emissions in the United States that have been estimated at ∼15,000 premature deaths annually[6,7] may be commensurately underestimated. Meanwhile, the U.S. EPA's NH_3 monitoring network (AMoN) is designed to measure NH_3 from agricultural sources and does not include any urban sites.[53] While previous studies based on in situ measurements have pointed out that vehicle emissions are an underestimated source of NH_3 in urban areas, it is laborious to use such approaches to monitor vehicle NH_3 emissions with extensive spatiotemporal coverage. Therefore, methods for tracking this urban source using remote sensing observations are valuable and essential. The range of top-down estimates provided here could be considerably reduced in future studies using formal inverse modeling techniques[54] or simultaneously estimating the trace gas lifetime from the satellite data itself.[37] These approaches would also account for the changes in meteorology in a more automated fashion than how they were considered here. Our approach also relied on estimates of changes in traffic activity, NO_x emissions, and the associated impacts on observed NO_2 column concentrations over regions not largely impacted by other sources; recognizing such information may not be readily available in all cities of interest, or that the separability of the traffic plume from additional sources may not be as facile, one could obtain estimates from inverse modeling studies that have estimated changes in NO_x emissions themselves.[55]

■ ASSOCIATED CONTENT

Supporting Information

The Supporting Information is available free of charge at https://pubs.acs.org/doi/10.1021/acs.estlett.1c00730.

Supporting figures and tables, rationale for the period selection, description of satellite observations and the FIVE inventory, details of our methods for estimating vehicle NH_3 emissions, analysis of meteorological impacts, estimates of bounds on the boundary flux entering the western LA box, and uncertainty analysis of our top-down vehicle NH_3 emissions estimates (PDF)

■ AUTHOR INFORMATION

Corresponding Author

Daven K. Henze − *Department of Mechanical Engineering, University of Colorado Boulder, Boulder, Colorado 80309, United States*; Phone: +1 303-492-8716; Email: daven.henze@colorado.edu; Fax: +1 303-492-3498

Authors

Hansen Cao − *Department of Mechanical Engineering, University of Colorado Boulder, Boulder, Colorado 80309, United States*; orcid.org/0000-0003-2713-0430

Karen Cady-Pereira − *Atmospheric and Environmental Research Inc., Lexington, Massachusetts 02421, United States*

Brian C. McDonald − *Chemical Sciences Laboratory, National Oceanic and Atmospheric Administration, Boulder, Colorado 80305, United States*; orcid.org/0000-0001-8600-5096

Colin Harkins − *Department of Mechanical Engineering, University of Colorado Boulder, Boulder, Colorado 80309, United States; Chemical Sciences Laboratory, National Oceanic and Atmospheric Administration, Boulder, Colorado 80305, United States; Cooperative Institute for Research in Environmental Sciences (CIRES), Boulder, Colorado 80309, United States*

Kang Sun − *Department of Civil, Structural and Environmental Engineering, University at Buffalo, Buffalo, New York 14260, United States*

Kevin W. Bowman − *Jet Propulsion Laboratory, California Institute of Technology, Pasadena, California 91109, United States*

Tzung-May Fu − *School of Environmental Science and Engineering, Southern University of Science and Technology, Shenzhen 518055, China*; orcid.org/0000-0002-8556-7326

Muhammad O. Nawaz − *Department of Mechanical Engineering, University of Colorado Boulder, Boulder, Colorado 80309, United States*

Complete contact information is available at: https://pubs.acs.org/10.1021/acs.estlett.1c00730

Notes

The authors declare no competing financial interest.

■ ACKNOWLEDGMENTS

This study is funded by NASA 80NSSC18K0689. The authors acknowledge NOAA for providing surface measurements of 2m temperature, precipitation, wind speed, and wind direction (available at ftp://ftp.ncdc.noaa.gov/pub/data/noaa/isd-lite/2020). The authors acknowledge the Tropospheric Monitoring Instrument (TROPOMI) group for providing offline total NO_2 column measurements (available at https://s5phub.copernicus.eu/dhus/#/home). The CrIS-SNPP NH_3 MUSES level-2 data (Standard product, including NH_3 profiles) is now publicly available at Earthdata (https://earthdata.nasa.gov). FIVE emissions (brian.mcdonald@noaa.gov) for March 2020 are available by request. The physics-based oversampling source code is available online (https://github.com/Kang-Sun-CfA/Oversampling_matlab/blob/master/popy.py). The GEOS-Chem v9-02 code coupled with the bidi scheme is available by request (daven.henze@Colorado.EDU). B.C.M. acknowledges the JPSS Proving Ground Risk Reduction Program and NOAA NRDD Project 19533. The authors thank Stuart McKeen (CIRES/NOAA CSL) for his help with processing the NEI 2017 emissions inventory. Part of this research was carried out at the Jet Propulsion Laboratory, California Institute of Technology as part of the TRopospheric Ozone and Its Precursors from Earth System Sounding (TROPESS) project under a contract with NASA. CrIS NH3 retrievals and diagnostics were processed courtesy of TROPESS (https://tes.jpl.nasa.gov/tropess/).

■ REFERENCES

(1) Sutton, M. A.; Erisman, J. W.; Dentener, F.; Möller, D. Ammonia in the environment: From ancient times to the present. *Environ. Pollut.* **2008**, *156*, 583−604.

(2) Moeckli, M. A.; Fierz, M.; Sigrist, M. W. Emission Factors for Ethene and Ammonia from a Tunnel Study with a Photoacoustic Trace Gas Detection System. *Environ. Sci. Technol.* **1996**, *30*, 2864−2867.

(3) Fraser, M. P.; Cass, G. R. Detection of Excess Ammonia Emissions from In-Use Vehicles and the Implications for Fine Particle Control. *Environ. Sci. Technol.* **1998**, *32*, 1053−1057.

(4) Huai, T.; Durbin, T. D.; Miller, J. W.; Pisano, J. T.; Sauer, C. G.; Rhee, S. H.; Norbeck, J. M. Investigation of NH3 Emissions from New Technology Vehicles as a Function of Vehicle Operating Conditions. *Environ. Sci. Technol.* **2003**, *37*, 4841−4847.

(5) Bishop, G. A.; Stedman, D. H. Reactive Nitrogen Species Emission Trends in Three Light-/Medium-Duty United States Fleets. *Environ. Sci. Technol.* **2015**, *49*, 11234−11240.

(6) Goodkind, A. L.; Tessum, C. W.; Coggins, J. S.; Hill, J. D.; Marshall, J. D. Fine-scale damage estimates of particulate matter air pollution reveal opportunities for locationspecific mitigation of emissions. *Proc. Natl. Acad. Sci. U. S. A.* **2019**, *116*, 8775−8780.

(7) Dedoussi, I. C.; Eastham, S. D.; Monier, E.; Barrett, S. R. Premature mortality related to United States cross-state air pollution. *Nature* **2020**, *578*, 261−265.

(8) Lurmann, F. W.; Hall, J. V.; Kleinman, M.; Chinkin, L. R.; Brajer, V.; Meacher, D.; Mummery, F.; Arndt, R. L.; Funk, T. H.; Alcorn, S. H.; Kumar, N. Assessment of the health benefits of improving air quality in Houston, Texas. City of Houston Office of the Mayor, November 1999.

(9) Kean, A. J.; Harley, R. A.; Littlejohn, D.; Kendall, G. R. On-road measurement of ammonia and other motor vehicle exhaust emissions. *Environ. Sci. Technol.* **2000**, *34*, 3535−3539.

(10) Sutton, M.; Dragosits, U.; Tang, Y.; Fowler, D. Ammonia emissions from nonagricultural sources in the UK. *Atmos. Environ.* **2000**, *34*, 855−869.

(11) Roe, S.; Spivey, M.; Lindquist, H.; Thesing, K.; Strait, R.; Pechan, E.; Associates, I. Estimating Ammonia Emissions from Anthropogenic Nonagricultural Sources. EPA Emission Inventory Improvement Program. Technical Report; Emission Inventory Improvement Program, 2004.

(12) Dore, C. J.; Watterson, J. D.; Murrells, T. P.; Passant, N. R.; Hobson, M. M.; Baggott, S. L.; Thistlethwaite, G.; Goodwin, J. W. L.; King, K. R.; Adams, M.; Walker, C.; Downes, M. K.; Coleman, P. J.; Stewart, R. A.; Wagner, A.; Sturman, J.; Conolly, C.; Lawrence, H.; Cumine, P. R. UK emissions of air pollutants 1970 to 2003. National Atmospheric Emissions Inventory, National Environmental Technology Centre, 2005.

(13) Livingston, C.; Rieger, P.; Winer, A. Ammonia emissions from a representative inuse fleet of light and medium-duty vehicles in the California South Coast Air Basin. *Atmos. Environ.* **2009**, *43*, 3326−3333.

(14) Pryor, S.; Anlauf, K.; Boudries, H.; Hayden, K.; Schiller, C.; Wiebe, A. Spatial and temporal variability of high resolution reduced nitrogen concentrations in the Fraser Valley. *Atmos. Environ.* **2004**, *38*, 5825−5836. (The Pacific 2001 Air Quality Study)

(15) Yao, X.; Hu, Q.; Zhang, L.; Evans, G. J.; Godri, K. J.; Ng, A. C. Is vehicular emission a significant contributor to ammonia in the urban atmosphere? *Atmos. Environ.* **2013**, *80*, 499−506.

(16) Suarez-Bertoa, R.; Mendoza-Villafuerte, P.; Riccobono, F.; Vojtisek, M.; Pechout, M.; Perujo, A.; Astorga, C. On-road measurement of NH3 emissions from gasoline and diesel passenger cars during real world driving conditions. *Atmos. Environ.* **2017**, *166*, 488−497.

(17) Felix, J. D.; Elliott, E. M.; Gish, T.; Maghirang, R.; Cambal, L.; Clougherty, J. Examining the transport of ammonia emissions across landscapes using nitrogen isotope ratios. *Atmos. Environ.* **2014**, *95*, 563−570.

(18) Kelly, J. T.; Baker, K. R.; Nowak, J. B.; Murphy, J. G.; Markovic, M. Z.; Vanden-Boer, T. C.; Ellis, R. A.; Neuman, J. A.; Weber, R. J.; Roberts, J. M.; Veres, P. R.; de Gouw, J. A.; Beaver, M. R.; Newman, S.; Misenis, C. Fine-scale simulation of ammonium and nitrate over the South Coast Air Basin and San Joaquin Valley of California during CalNex-2010. *Journal of Geophysical Research: Atmospheres* **2014**, *119*, 3600−3614.

(19) Sun, K.; Tao, L.; Miller, D. J.; Pan, D.; Golston, L. M.; Zondlo, M. A.; Griffin, R. J.; Wallace, H. W.; Leong, Y. J.; Yang, M. M.; Zhang, Y.; Mauzerall, D. L.; Zhu, T. Vehicle Emissions as an Important Urban Ammonia Source in the United States and China. *Environ. Sci. Technol.* **2017**, *51*, 2472−2481.

(20) Fenn, M. E.; Bytnerowicz, A.; Schilling, S. L.; Vallano, D. M.; Zavaleta, E. S.; Weiss, S. B.; Morozumi, C.; Geiser, L. H.; Hanks, K. On-road emissions of ammonia: An underappreciated source of atmospheric nitrogen deposition. *Sci. Total Environ.* **2018**, *625*, 909−919.

(21) Berner, A. H.; Felix, J. D. Investigating ammonia emissions in a coastal urban airshed using stable isotope techniques. *Sci. Total Environ.* **2020**, *707*, 134952.

(22) David Felix, J.; Elliott, E. M.; Gish, T. J.; McConnell, L. L.; Shaw, S. L. Characterizing the isotopic composition of atmospheric ammonia emission sources using passive samplers and a combined oxidation-bacterial denitrifier approach. *Rapid Commun. Mass Spectrom.* **2013**, *27*, 2239−2246.

(23) Zhang, Y.; Liu, X.; Fang, Y.; Liu, D.; Tang, A.; Collett, J. L. Atmospheric Ammonia in Beijing during the COVID-19 Outbreak: Concentrations, Sources, and Implications. *Environ. Sci. Technol. Lett.* **2021**, *8*, 32−38.

(24) Whitehead, J.; Longley, I.; Gallagher, M. Seasonal and diurnal variation in atmospheric ammonia in an urban environment measured using a quantum cascade laser absorption spectrometer. *Water, Air, Soil Pollut.* **2007**, *183*, 317−329.

(25) Chang, Y.; Zou, Z.; Deng, C.; Huang, K.; Collett, J. L.; Lin, J.; Zhuang, G. The importance of vehicle emissions as a source of atmospheric ammonia in the megacity of Shanghai. *Atmos. Chem. Phys.* **2016**, *16*, 3577−3594.

(26) Sun, K.; Tao, L.; Miller, D. J.; Khan, M. A.; Zondlo, M. A. On-Road Ammonia Emissions Characterized by Mobile, Open-Path Measurements. *Environ. Sci. Technol.* **2014**, *48*, 3943−3950.
(27) Thiruvengadam, A.; Besch, M.; Carder, D.; Oshinuga, A.; Pasek, R.; Hogo, H.; Gautam, M. Unregulated greenhouse gas and ammonia emissions from current technology heavy-duty vehicles. *J. Air Waste Manage. Assoc.* **2016**, *66*, 1045−1060.
(28) Miller, D. J.; Sun, K.; Tao, L.; Khan, M. A.; Zondlo, M. A. Open-path, quantum cascade-laser-based sensor for high-resolution atmospheric ammonia measurements. *Atmos. Meas. Tech.* **2014**, *7*, 81−93.
(29) Farren, N. J.; Davison, J.; Rose, R. A.; Wagner, R. L.; Carslaw, D. C. Underestimated Ammonia Emissions from Road Vehicles. *Environ. Sci. Technol.* **2020**, *54*, 15689−15697.
(30) Nowak, J. B.; Neuman, J. A.; Bahreini, R.; Middlebrook, A. M.; Holloway, J. S.; McKeen, S. A.; Parrish, D. D.; Ryerson, T. B.; Trainer, M. Ammonia sources in the California South Coast Air Basin and their impact on ammonium nitrate formation. *Geophys. Res. Lett.* **2012**, *39*, n/a.
(31) Pinder, R. W.; Walker, J. T.; Bash, J. O.; Cady-Pereira, K. E.; Henze, D. K.; Luo, M.; Osterman, G. B.; Shephard, M. W. Quantifying spatial and seasonal variability in atmospheric ammonia with in situ and space-based observations. *Geophys. Res. Lett.* **2011**, *38*, n/a.
(32) Warner, J. X.; Dickerson, R. R.; Wei, Z.; Strow, L. L.; Wang, Y.; Liang, Q. Increased atmospheric ammonia over the world's major agricultural areas detected from space. *Geophys. Res. Lett.* **2017**, *44*, 2875−2884.
(33) Van Damme, M.; Clarisse, L.; Whitburn, S.; Hadji-Lazaro, J.; Hurtmans, D.; Clerbaux, C.; Coheur, P.-F. Industrial and agricultural ammonia point sources exposed. *Nature* **2018**, *564*, 99.
(34) Alvarado, M. J.; Cady-Pereira, K. E.; Xiao, Y.; Millet, D. B.; Payne, V. H. Emission ratios for ammonia and formic acid and observations of peroxy acetyl nitrate (PAN) and ethylene in biomass burning smoke as seen by the tropospheric emission spectrometer (TES). *Atmosphere* **2011**, *2*, 633−654.
(35) Clarisse, L.; Van Damme, M.; Clerbaux, C.; Coheur, P.-F. Tracking down global NH3 point sources with wind-adjusted super resolution. *Atmos. Meas. Tech.* **2019**, *12*, 5457−5473.
(36) Zhou, C.; Zhou, H.; Holsen, T. M.; Hopke, P. K.; Edgerton, E. S.; Schwab, J. J. Ambient Ammonia Concentrations Across New York State. *J. Geophys. Res.: Atmos.* **2019**, *124*, 8287−8302.
(37) Goldberg, D. L.; Anenberg, S. C.; Griffin, D.; McLinden, C. A.; Lu, Z.; Streets, D. G. Disentangling the Impact of the COVID-19 Lockdowns on Urban NO2 From Natural Variability. *Geophys. Res. Lett.* **2020**, *47*, No. e2020GL089269.
(38) Shephard, M. W.; Cady-Pereira, K. E.; Luo, M.; Henze, D. K.; Pinder, R. W.; Walker, J. T.; Rinsland, C. P.; Bash, J. O.; Zhu, L.; Payne, V. H.; Clarisse, L. TES ammonia retrieval strategy and global observations of the spatial and seasonal variability of ammonia. *Atmos. Chem. Phys.* **2011**, *11*, 10743−10763.
(39) Shephard, M. W.; Cady-Pereira, K. E. Cross-track Infrared Sounder (CrIS) satellite observations of tropospheric ammonia. *Atmos. Meas. Tech.* **2015**, *8*, 1323−1336.
(40) Fu, D.; Kulawik, S. S.; Miyazaki, K.; Bowman, K. W.; Worden, J. R.; Eldering, A.; Livesey, N. J.; Teixeira, J.; Irion, F. W.; Herman, R. L.; Osterman, G. B.; Liu, X.; Levelt, P. F.; Thompson, A. M.; Luo, M. Retrievals of tropospheric ozone profiles from the synergism of AIRS and OMI: methodology and validation. *Atmos. Meas. Tech.* **2018**, *11*, 5587−5605.
(41) van Geffen, J.; Boersma, K.; Van Roozendael, M.; Hendrick, F.; Mahieu, E.; De Smedt, I.; Sneep, M.; Veefkind, J. Improved spectral fitting of nitrogen dioxide from OMI in the 405−465 nm window. *Atmos. Meas. Tech.* **2015**, *8*, 1685−1699.
(42) van Geffen, J.; Eskes, H.; Boersma, K.; Maasakkers, J.; Veefkind, J. TROPOMI ATBD of the total and tropospheric NO2 data products. KNMI, 2019 (https://sentinels.copernicus.eu/documents/247904/2476257/Sentinel-5P-TROPOMI-ATBD-NO2-data-products, accessed 2021-11-04).
(43) Sun, K.; Zhu, L.; Cady-Pereira, K.; Chan Miller, C.; Chance, K.; Clarisse, L.; Coheur, P.-F.; González Abad, G.; Huang, G.; Liu, X.; Van Damme, M.; Yang, K.; Zondlo, M. A physics-based approach to oversample multi-satellite, multispecies observations to a common grid. *Atmos. Meas. Tech.* **2018**, *11*, 6679−6701.
(44) McDonald, B. C.; McBride, Z. C.; Martin, E. W.; Harley, R. A. High-resolution mapping of motor vehicle carbon dioxide emissions. *Journal of Geophysical Research: Atmospheres* **2014**, *119*, 5283−5298.
(45) Kim, S.-W.; McDonald, B. C.; Baidar, S.; Brown, S. S.; Dube, B.; Ferrare, R. A.; Frost, G. J.; Harley, R. A.; Holloway, J. S.; Lee, H.-J.; McKeen, S. A.; Neuman, J. A.; Nowak, J. B.; Oetjen, H.; Ortega, I.; Pollack, I. B.; Roberts, J. M.; Ryerson, T. B.; Scarino, A. J.; Senff, C. J.; et al. Modeling the weekly cycle of NOx and CO emissions and their impacts on O3 in the Los Angeles-South Coast Air Basin during the CalNex 2010 field campaign. *Journal of Geophysical Research: Atmospheres* **2016**, *121*, 1340−1360.
(46) McDonald, B. C.; McKeen, S. A.; Cui, Y. Y.; Ahmadov, R.; Kim, S. W.; Frost, G. J.; Pollack, I. B.; Peischl, J.; Ryerson, T. B.; Holloway, J. S.; Graus, M.; Warneke, C.; Gilman, J. B.; de Gouw, J. A.; Kaiser, J.; Keutsch, F. N.; Hanisco, T. F.; Wolfe, G. M.; Trainer, M. Modeling Ozone in the Eastern US using a Fuel-Based Mobile Source Emissions Inventory. *Environ. Sci. Technol.* **2018**, *52*, 7360−7370.
(47) Highway Statistics 2019, Table MF-2: Motor-Fuel Vol. Taxed by States. Office of Highway Policy Information. Federal Highway Administration, U.S. Department of Transportation: Washington, DC, 2020.
(48) Worldwide Syngas Database. 2020.
(49) Dammers, E.; McLinden, C. A.; Griffin, D.; Shephard, M. W.; Van Der Graaf, S.; Lutsch, E.; Schaap, M.; Gainairu-Matz, Y.; Fioletov, V.; Van Damme, M.; Whitburn, S.; Clarisse, L.; Cady-Pereira, K.; Clerbaux, C.; Coheur, P. F.; Erisman, J. W. NH3 emissions from large point sources derived from CrIS and IASI satellite observations. *Atmos. Chem. Phys.* **2019**, *19*, 12261−12293.
(50) Lelieveld, J.; Evans, J. S.; Fnais, M.; Giannadaki, D.; Pozzer, A. The contribution of outdoor air pollution sources to premature mortality on a global scale. *Nature* **2015**, *525*, 367−371.
(51) Giannakis, E.; Kushta, J.; Giannadaki, D.; Georgiou, G. K.; Bruggeman, A.; Lelieveld, J. Exploring the economy-wide effects of agriculture on air quality and health: evidence from Europe. *Sci. Total Environ.* **2019**, *663*, 889−900.
(52) Zhang, X.; Gu, B.; van Grinsven, H.; Lam, S. K.; Liang, X.; Bai, M.; Chen, D. Societal benefits of halving agricultural ammonia emissions in China far exceed the abatement costs. *Nat. Commun.* **2020**, *11*, 4357.
(53) *Ammonia Monitoring Network Site Operations Manual*; NADP Program Office, 2015.
(54) Cao, H.; Henze, D. K.; Shephard, M. W.; Dammers, E.; Cady-Pereira, K.; Alvarado, M.; Lonsdale, C.; Luo, G.; Yu, F.; Zhu, L.; Danielson, C. G.; Edgerton, E. S. Inverse modeling of NH3 sources using CrIS remote sensing measurements. *Environ. Res. Lett.* **2020**, *15*, 104082.
(55) Miyazaki, K.; Bowman, K.; Sekiya, T.; Jiang, Z.; Chen, X.; Eskes, H.; Ru, M.; Zhang, Y.; Shindell, D. Air Quality Response in China Linked to the 2019 Novel Coronavirus (COVID-19) Lockdown. *Geophys. Res. Lett.* **2020**, *47*, n/a.